PHYSICAL REVIEW B **74**, 121201(R) (2006)

Prediction of the anomalous fluorine-silicon interstitial pair diffusion in crystalline silicon

Scott A. Harrison, Thomas F. Edgar, and Gyeong S. Hwang*
Department of Chemical Engineering, University of Texas, Austin, Texas 78713, USA
(Received 24 April 2006; revised manuscript received 5 July 2006; published 6 September 2006)

We propose a diffusion pathway for a fluorine-silicon interstitial pair (F-Si_i) in silicon based on extensive first-principles density functional calculations. We find the F-Si_i pair to be most stable in the singly positive charge state under intrinsic conditions and can exist in nearly degenerate bound and unbound states. We determine that the unbound pair can undergo diffusion with a barrier of approximately 0.4–0.5 eV by a coordinated motion until dissociating into F and Si interstitials at a cost of 1.3 eV. Our results suggest that Si interstitials, when they exist in excess, can play an important role in F redistribution and precipitation during thermal treatments.

DOI: 10.1103/PhysRevB.74.121201 PACS number(s): 61.72.−y, 66.30.−h

A deeper understanding of the atomic-level behavior of dopants, impurities, and defects has become more important in designing experiments to realize the formation of ever shallower and more abrupt junctions with higher doping levels for the 45-nm node or beyond. Currently ultra-low-energy ion implantation followed by rapid thermal annealing is most widely used for ultrashallow junction formation, while other alternative technologies such as laser annealing suffer from significant process integration challenges. During the post-implantation annealing step, implanted dopants often undergo significant transient enhanced diffusion (TED), which in turn hinders the formation of ultrashallow junctions. In addition, defect-mediated dopant clustering often limits the achievement of desired dopant electrical activation levels. In recent years, coimplantation of fluorine (F) with dopants has become a viable strategy to reduce dopant TED and deactivation. However, the role of intrinsic defects in the redistribution of implanted F atoms is still ambiguous, despite its importance given the abundant existence of mobile interstitials (Si_i) and vacancies (V) during postimplantation annealing. While recent experiments have demonstrated the formation of F-V complexes,[1,2] there is a lack of understanding regarding the interaction between F and Si_i.

Current understanding attributes F diffusion in Si primarily to the migration of interstitial F from a bond-centered site (F_{bc}) or a tetrahedral site (F_{tet}), depending on the Fermi level energy.[3] However, earlier experimental studies have suggested the importance of mobile F-Si interstitial (F-Si_i) complexes in explaining F behavior in crystalline Si. Pi *et al.*[4] attributed the dissolution of F precipitates in both interstitial and vacancy rich regions to the transient diffusion of F-Si_i complexes during thermal annealing. Park and Kim (Ref. 5) suggested the formation and diffusion of F-Si_i pairs to explain suppression of large Si cluster formation. Recently, Robison and Law (Ref. 6) also suggested that Si interstitials may play an important role in determining F redistribution during postimplantation annealing. On the other hand, a recent theoretical study[7] suggested that a stable F-Si_i pair could form in the positive charge state, but was determined to be immobile. Despite strong experimental indication that Si interstitials can affect F redistribution, no clear description of their role in F diffusion is available.

In this paper, the structure, stability, and diffusion F-Si_i pairs are presented based on density functional calculations. Our calculations predict the formation of stable F-Si_i pairs that can undergo diffusion with a moderate barrier (of 0.4–0.5 eV), providing theoretical support for the earlier experimental prediction of the important role of F-Si_i pairs in F redistribution.[4–6]

All atomic structures and energies reported herein were calculated within the generalized gradient approximation [PW91 (Ref. 8)] to density functional theory (DFT) using the well established Vienna *ab initio* simulation package (VASP).[9] A plane-wave basis set for valence electron states and Vanderbilt ultrasoft pseudopotentials[10] for core-electron interactions were employed. A plane-wave cutoff energy of 320 eV was used. The Brillouin zone integration was performed using a $(2\times2\times2)$ mesh of k points in the scheme of Monkhorst-Pack. We checked carefully the convergence of atomic configurations and relative energies with respect to the cutoff energy and the k-point mesh. All defect systems examined here were modeled using 64-atom supercells with a fixed lattice constant of 5.457 Å. All atoms were fully relaxed using the conjugate gradient method until residual forces on constituent atoms become smaller than 5×10^{-2} eV/Å. Diffusion barriers and pathways were computed using the nudged elastic band method (NEBM). In applying this method, eight intermediate images were used to determine the converged minimum energy paths between adjacent local energy minimums. For a few selected defect-dopant complexes, bonding mechanisms were also analyzed using the electron localization function (ELF) that represents the electron pair localization in terms of the conditional probability of finding an electron in the neighborhood of another electron with the same spin.[11] An ELF can take on values between 0 and 1, where an ELF equal to 1 corresponds to perfect electron pair localization and an ELF equal to $\frac{1}{2}$ corresponds to a homogeneous electron gaslike pair probability.

The relative stability of neutral and charged defects was assessed by computing defect ionization levels (μ_i). At a given Fermi level (ϵ_F), the relative formation energy of a charged defect in charge state $q=\pm1$ to a neutral defect is given by $E_f^q-E_f^0=q(\epsilon_F-\mu_i)$, where ϵ_F is given relative to the valence band maximum (E_V). The defect levels can be approximated by: $E_D^q+q(E_v^q+\mu_i)=E_D^0$, where E_D^q and E_D^0

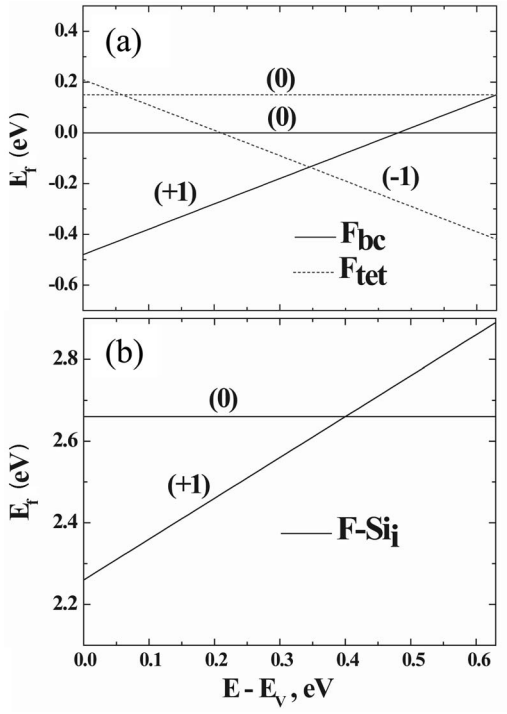

FIG. 1. Variation in the relative formation energies of (a) interstitial F (b) F-Si$_i$, with respect to F_{bc}^0 as a function of the Fermi energy (ε_F) for the computed Si gap of 0.63 eV.

are the total energies of the defects in q and neutral charge states, and E_v^q is the position of the valence band maximum in supercell E_D^q. In calculating a charged defect, a homogeneous background charge is included to maintain the overall charge neutrality in the periodic supercell. To account for the Coulomb energy between the charged defect and the background charge, a monopole correction is made to the total energy of the charged system.[12] Assuming a pointlike +1 charge defect in the 64-atom supercell, the monopole correction is estimated to be approximately 0.16 eV. This correction may be larger than the required adjustment if the charge on the defect is significantly delocalized.[13]

For the sake of reference we first calculated the relative formation energies of interstitial F at different configurations and charge states, with respect to neutral (bond centered) F (F_{bc}^0). Figure 1(a) shows the relative formation energies of F atoms at the bond-centered (F_{bc}) and tetrahedral (F_{tet}) interstitial sites as a function of the Fermi energy. For the computed gap of 0.63 eV, F_{bc}^+ is predicted to be the lowest energy structure up to a Fermi level of 0.35 eV, after which F_{tet}^- becomes the most favorable configuration energetically, in good agreement with earlier DFT studies.[3,7] Similarly, we then calculated the relative formation energies of F-Si$_i$ pairs in neutral and positive charge states, as shown in Fig. 1(b). Here, we only considered the (unbound) structure where the F and Si interstitials are not directly connected (see Fig. 2), which is energetically nearly degenerate with another competing local-minimum (bound) structure where the F and Si interstitials are in direct contact with each other [see Fig. 3(d)]. Considering the computed Si gap, the positively-charged F-Si$_i$ pair is found to be the most stable pair in

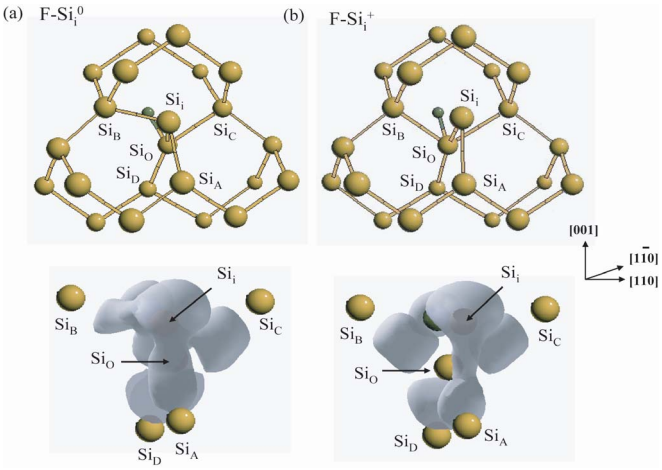

FIG. 2. (Color online) (Upper panel) Lowest-energy structures of (a) F-Si$_i^0$ and (b) F-Si$_i^+$ (Lower panel) Electron localization functions (ELFs) of the corresponding F-Si$_i$ complexes. The value of the ELF isosurfaces is set at 0.75. The small dark gray (green) and large gray (yellow) balls represent F and Si atoms, respectively.

intrinsic regions, consistent with previous theoretical studies.[7] We also examined the negatively charged F-Si$_i$ pair, but it was found to be far less energetically favorable than the neutral and positive ones under intrinsic conditions.

Figure 2 (lower panels) shows the ELF isosurfaces for the neutral and positive (unbound) F-Si$_i$ pairs, which may also assist in understanding why the positively changed F-Si$_i$ pair can be energetically more favorable than the neutral pair. For F-Si$_i^0$, the center lattice Si atom (Si$_O$) is bonded to two

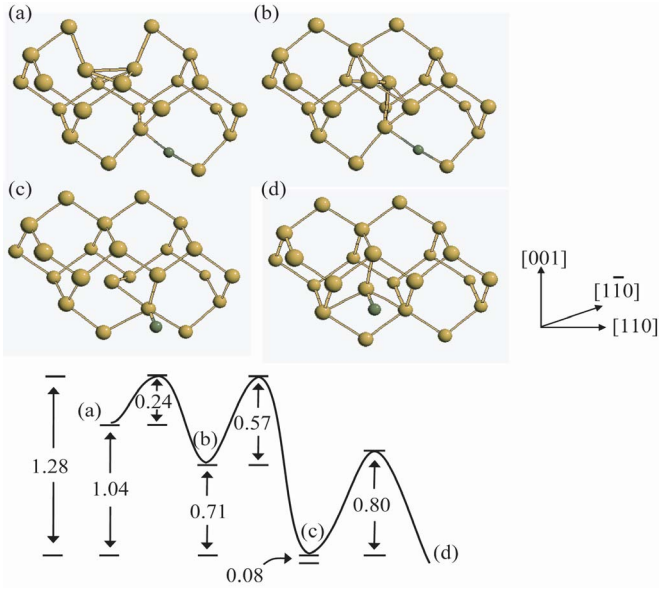

FIG. 3. (Color online) (Upper panel) Formation mechanism for F-Si$_i^+$ including (a) separate Si$_i$ and bond-centered F interstitial, (b) an approximate tetrahedral Si$_i$ adjacent to a bond-centered F interstitial, (c) an unbound F-Si$_i^+$ pair, and (d) a bound F-Si$_i^+$ pair. The small dark gray (green) and large gray (yellow) balls represent F and Si atoms, respectively. (Lower panel) Energetics (in eV) along the F-Si$_i^+$ formation pathway.

neighboring lattice Si atoms (Si_C, Si_D), the interstitial Si atom (Si_i), and the F atom, while Si_i is bonded to Si_O, Si_A, and Si_B in the sp^3 configuration. (Note that Si_O was initially connected to Si_A, Si_B, Si_C, and Si_D.) From the plot of ELF isosurfaces, it can be noted that the Si-Si bonds associated with F-Si_i^0 are highly distorted, which in turn results in high strain energy. For F-Si_i^+, on the other hand, Si_O is covalently bonded to Si_B, Si_C, Si_D, in the sp^2 configuration, and forms an ionic bond with F that results from charge transfer from Si_O to F. Additionally, the ELF isosurface [Fig. 2(b)] demonstrates the formation of a polar covalent bond between Si_i and Si_A, with a greater amount of bonding electrons towards Si_A. This bonding structure leaves a lone electron pair on Si_i, and also results in less strain than the neutral structure.

Taking the predicted relative formation energies (Fig. 1), the binding energy of the F-Si_i^+ pair is predicted to be 0.95 eV at mid-gap, relative to the dissociation products F_{bc}^+ and (110)-split Si_i^0. Here, the F-Si_i^+ binding energy is given by: $E_b(\text{F-Si}_i^+)=E_f(\text{F}_{bc}^+)+E_f(\text{Si}_i^0)-E_f(\text{F-Si}_i^+)$, where $E_f(\text{Si}_i^0)$ is the (110)-split Si_i^0 formation energy which is estimated to be 3.69 eV. Since uncertainty still exists in the DFT values of the ionization levels and consequently the relative formation energies of charged defects at a given Fermi energy, we should mention that the absolute values of the F-Si_i binding energies are subject to this inherent error. Nonetheless our result at least demonstrates the existence of stable F-Si_i complexes in Si.

Next we examined mechanisms for the formation and diffusion of F-Si pairs. Figure 3 shows a viable route that we have identified for F-Si^+ pair formation, starting from a (110)-split Si_i and a bond centered F (F_{bc}). Here, each supercell contains a single positive charge. In (a), a (110)-split Si_i approaches to F_{bc} and overcomes an association barrier of 0.24 eV to form (b) where the Si_i lies in an approximate tetrahedral position adjacent to F_{bc}. From (b), the Si_i overcomes a 0.57 eV barrier to form the unbound F-Si_i^+ pair [(c)]. The unbound F-Si_i^+ pair is found to undergo transformation to the bound F-Si_i^+ pair [(d)] with a barrier of 0.80 eV. The bound and unbound structures of F-Si_i^+ are consistent with recent DFT results.[5] However, the energy barrier for the bound to unbound transformation was predicted to be 1.4 eV, leading to the conclusion that the F -Si_i^+ pair is immobile. Through extensive search, we have identified a minimum-energy pathway with a barrier of 0.80 eV from the bound to unbound state. Given their degeneracy and sizable dissociation barriers we expect that the bound and unbound complex concentrations will be similar.

Figure 4 shows the local minima and saddle points (upper panel), together with the total energy variations along the lowest energy path identified for F-Si_i^+ migration (lower panel), starting from the unbound configuration. In the initial diffusion step from (a) to (c), F diffuses at a cost of 0.49 eV between neighboring lattice Si atoms through a transition state (b). This step is followed by the reorientation of F from (c) to (d) which has a smaller barrier of 0.18 eV. The overall diffusion barrier is predicted to be 0.49 eV. For the saddle configuration (b), the Si_i is in a hexagonal site with F equidistant between neighboring lattice Si atoms. To achieve the saddle configuration (b), there is an evident coordinated motion between the F and Si interstitial that allows the two atoms to diffuse as a pair.

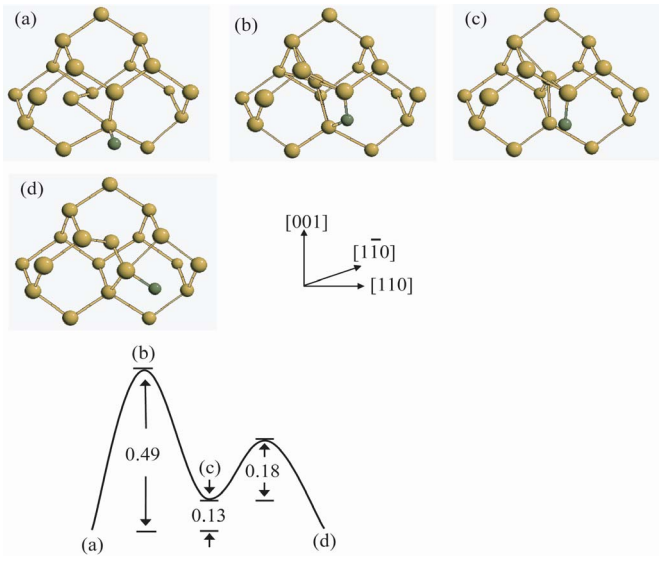

FIG. 4. (Color online) (Upper panel) Diffusion mechanism for F-Si_i^+ starting from the unbound configuration. The small dark gray (green) and large gray (yellow) balls represent F and Si atoms respectively. (Lower panel) Energetics (in eV) along the F-Si_i^+ diffusion pathway.

Figure 5 shows the atomic structures of the local minima and saddle points (upper panel), together with the energy changes along the lowest-energy path for F-Si_i^0 diffusion (lower panel). The diffusion mechanism for the F-Si_i^0 pair is distinctly different from that of the F-Si_i^+ pair. In the neutral case, the Si_i is able to assume the position of a [100] Si interstitial in (b) at an energy cost of only 0.13 eV prior to the transfer of the F to a Si neighbor [as shown in (c)] by overcoming a barrier of only 0.07 eV. Once the F is transferred to a new Si atom, it undergoes two successive reori-

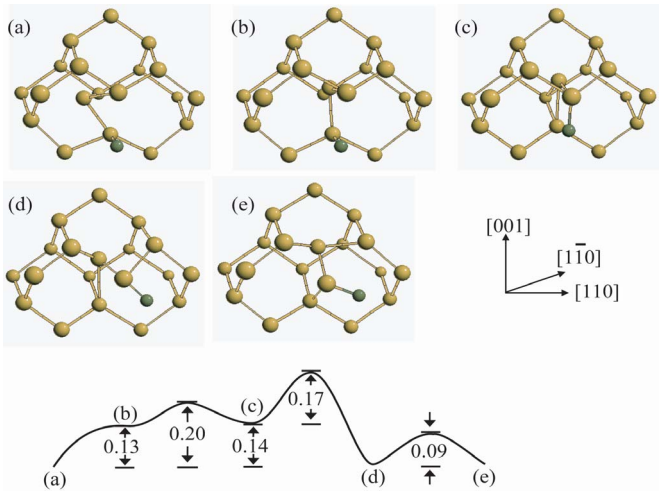

FIG. 5. (Color online) (Upper panel) Diffusion mechanism for F-Si_i, starting from the unbound configuration. The small dark gray (green) and large gray (yellow) balls represent F and Si atoms respectively. (Lower panel) Energetics (in eV) along the F-Si_i diffusion pathway.

entations from (c) to (d) and (d) to (e) at costs of 0.17 eV and 0.09 eV, respectively. Under the steady-state approximation, the overall barrier is then calculated to be 0.31 eV, about 0.18 eV lower than the positively charged case. Allowing a charge variation from F-Si_i^+ to F-Si_i^0 under intrinsic conditions, which has a 0.1 eV higher formation energy than F -Si_i^+, yields in total a diffusion barrier of about 0.4 eV for the migration process F-$Si_i^+ \rightarrow$ F-$Si_i^0 \rightarrow$ F-Si_i^+.

In summary, based on our theoretical results, we propose a mechanism for Si interstitial-mediated F diffusion which involves: (i) the binding of a mobile F and mobile Si interstitial to form a F-Si_i pair which will oscillate between the bound and unbound states; and (ii) the unbound pair undergoing diffusion by coordinated motion between F and Si interstitial until it dissociates into F and Si interstitials or reconfigures into the bound pair. Taking the computed gap of 0.63 eV, the dissociation and diffusion barriers of the most stable F-Si_i^+ pair are predicted to be approximately 1.3 eV and 0.5 eV (or 0.4 eV if charge variation allowed during diffusion), respectively, under intrinsic conditions. F-Si_i^+ pairs are likely to be as mobile as F interstitials given that F_{tet}^- has been predicted to diffuse with a barrier of 0.60 eV, which is far lower than the 1.38 eV migration barrier for F_{bc}^+ diffusion.[3] Note that F_{tet}^- and F_{bc}^+ are approximately equal in energy at mid-gap [see Fig. 2(b)]. The moderate diffusion barrier relative to the high dissociation barrier suggests that Si interstitials, when they exist in excess, can play an important role in F diffusion, irrespective of some possible error in DFT calculations of their values.

G.S.H. greatly acknowledges the Welch Foundation (F-1535) and the National Science Foundation (CAREER-CTS-0449373 and ECS-0304026) for their partial financial support. S.A.H. would like to thank the NSF and the University of Texas for financial support. We would also like to thank the Texas Advanced Computing Center for use of their computing resources.

*Author to whom correspondence should be addressed. Email address: gshwang@che.utexas.edu

[1] H. A. W. El Mubarek and P. Ashburn, Appl. Phys. Lett. **83**, 4134 (2003).
[2] X. D. Pi, C. P. Burrows, and P. G. Coleman, Phys. Rev. Lett. **90**, 155901 (2003).
[3] M. Diebel and S. T. Dunham, Phys. Rev. Lett. **93**, 245901 (2004).
[4] X. D. Pi, C. P. Burrows, and P. G. Coleman, Phys. Rev. Lett. **90**, 155901 (2003).
[5] Y. J. Park and J. J. Kim, J. Appl. Phys. **85**, 803 (1999).
[6] R. R. Robison, A. F. Saavedra, and M. E. Law, Mater. Res. Soc. Symp. Proc. **810**, 365 (2004).
[7] G. M. Lopez, V. Fiorentini, G. Impellizzeri, S. Mirabella, and E. Napolitani, Phys. Rev. B **72**, 045219 (2005).
[8] J. P. Perdew and Y. Wang, Phys. Rev. B **45**, 13244 (1992).
[9] G. Kresse and J. Furthmuller, *VASP the Guide* (Vienna University of Technology, Vienna, 2001); G. Kresse and J. Hafner, Phys. Rev. B **47**, 558 (1993); G. Kresse and J. Furthmuller, Comput. Mater. Sci. **6**, 15 (1996); G. Kresse and J. Furthmuller, Phys. Rev. B **54**, 11169 (1996).
[10] D. Vanderbilt, Phys. Rev. B **41**, 7892 (1990).
[11] A. D. Becke and K. E. Edgecombe, J. Chem. Phys. **92**, 5397 (1990).
[12] G. Makov and M. C. Payne, Phys. Rev. B **51**, 4014 (1995).
[13] D. Segev and S. H. Wei, Phys. Rev. Lett. **91**, 126406 (2003).